Send Orders for Reprints to reprints@benthamscience.ae

32 *Open Chemistry Journal*, 2018, *5*, 32-43

BENTHAM OPEN

CrossMark

Open Chemistry Journal

Content list available at: www.benthamopen.com/CHEM/

DOI: 10.2174/1874842201805010032

RESEARCH ARTICLE

The Synthesis of a Novel Anticancer Compound, *N*-(3,5 Dimethoxyphenyl) Acridin-9-Amine and Evaluation of Its Toxicity

Nur A. Ismail[1], Abbas A. Salman[1], Mohd S. M. Yusof[2], Siti K. C. Soh[3], Hapipah M. Ali[1] and Rozie Sarip[1,*]

[1]*Department of Chemistry, Faculty of Science, University of Malaya, Lembah Pantai, 50603 Kuala Lumpur, Malaysia*
[2]*School of Fundamental Sciences, Universiti Malaysia Terengganu, 21030 Kuala Nerus, Terengganu, Malaysia*
[3]*School of Marine and Environmental Sciences, Universiti Malaysia Terengganu, 21030 Kuala Nerus, Terengganu, Malaysia*

Received: December 26, 2017 Revised: February 13, 2018 Accepted: April 8, 2018

Abstract:

Introduction:

Acridine is a class of organic compounds which offers a wide range of biological and physical properties due to its unique chemical skeleton. A lot of researches have focused on the moulding of the substituents of the acridine ring system in an attempt to enhance its biological applications, especially in terms of anticancers, antioxidants, and antivirals.

Materials and Methods:

In this study, a new compound *N*-(3,5-dimethoxyphenyl)acridin-9-amine (G4) was synthesized through the Ullmann condensation of 2-chlorobenzoic acid and 3,5-dimethoxyaniline. *In vitro* cytotoxicity investigations of G4 on normal cell (WRL 68) and cancer cell lines (MCF-7, HT29 and HL60) were then conducted. *In vivo* evaluation or acute toxicology, was also carried out whereby male and female mice were administered G4 orally in single doses of 0 (control group), 500, and 1000 mg/kg.

Results:

As per the results, G4 exhibited *in vitro* antiproliferative activity on all the cancer cell lines tested. Also, no signs of toxicity were observed in the mice even after being administered the highest dose of G4. The structure of the compound was determined by single crystal X-ray diffraction analysis, CHN elemental analysis, Fourier Transformed Infrared (FTIR), ^{1}H nuclear magnetic resonance (NMR), and ^{13}C attached proton test (APT) NMR. G4 was found to be slightly planar and in discrete asymmetric units.

Conclusion:

The acridine was observed to be bound to 3,5-dimethoxyaniline (N1) as the confirmed **G4** molecule. Also, the exocyclic carbon at position C13 was found to be monodentate and slightly planar. **G4** exhibited profound antiproliferative activity towards HL60 cancer cell lines.

Keywords: Acridine, Heterocycle, *N*-(3,5- Dimethoxyphenyl)acridin-9-amine, Acute toxicity, Antiproliferative, Anticancers.

1. INTRODUCTION

Acridine is a class of organic compounds known as π-electron-deficient heterocycles that possess a number of unique chemical and physical properties [1]. It is also widely reported that acridine an *N*-donor ligand, has a high tendency to cyclometallate compounds, especially those of heavy metals such as platinum [2] and palladium [3].

* Address correspondence to this author at the Department of Chemistry, Faculty of Science, University of Malaya, Lembah Pantai, 50603 Kuala Lumpur, Malaysia; Tel: +603 7967 7022; E-mail: rozie@um.edu.my

The biological activity of acridine can primarily be attributed to its core structure a benzene ring and either $–NHCH_2-$ or $–NHCH_2CH_2-$ [4]. Moreover, the other substituents that attach to acridine especially 9-anilinacridine [5], are proven to be able to enhance the biological potency of acridine and reduce its side effects following interaction with DNA [6]. Hence, the modification of acridine either by metallation or by changing its substituents is an interesting field for researchers in their quest to discover new potent anticancer agents.

Nowadays, cancer is one of the major diseases [7] which results in mortality, and its occurrence is increasing by the year. In 2012, about 14 million new cancer cases have been reported worldwide, 2.2 million (15.4%) of which were due to carcinogenic infections [8]. In medical science, acridine is a chemical with anticancer activity [9] and is used as an antileukemic agent, for instance [10]. This is in light of the interactions between its π-π system and the base pairs of double-stranded DNA, notwithstanding the high affinity of the latter for the former. Furthermore, amsacrine (m-AMSA), an acridine derivative, was the first known DNA-intercalating agent, or topoisomerase II inhibitor [6b].

Acridine also possesses a wide range of other biological activities, which include antibacterial [11], trypanocidal [12], and antimalarial [13] activities. Additionally, this compound has various other applications. For example, the fluorescence of acridine (AO) [14] allows the detection of tumors, metasteses, and residual disease after surgical excision [15]. Meanwhile, acridine yellow is used as a dye-like biomolecule [16] in numerous photosensitizer studies. An example is a research on solar cell production [17], in which acridine yellow is involved in the synthesis of TiO_2 films containing nanosized semiconductor particles.

In this research, we report the anticancer activity of *N*-(3,5- dimethoxyphenyl)acridin-9-amine (**G4**), which has been studied *in vitro* as well as *in vivo*. When the methoxy functional group was added to acridine, the anticancer activity of the derivative was enhanced, thus allowing it to be further developed as a chemotherapeutic drug [18].

2. MATERIALS AND METHODS

2.1. Materials and Instrumentals

The chemicals and solvents were obtained from Merck, Sigma-Aldrich, and Fisher Scientific, and were used without further purification unless stated otherwise. The infrared spectra of the synthesized compounds were measured using a Perkin Elmer Spectrum One FT-IR spectrophotometer (ATR) within the wavelength range of 450 – 4000 cm^{-1}. The ^{1}H and ^{13}C-APT Nuclear Magnetic Resonance (NMR) spectra were determined by an AVN Bruker 400 FT-NMR and Jeol ECX DELTA 400 MHz spectroscope, with deuterated chloroform as the solvent. Elemental analysis of the carbon, hydrogen, and nitrogen (CHN) compositions were performed using a Perkin Elmer CHNS/O 2400 series II elemental analyser. The single crystal X-ray diffraction data of some of the complexes were assessed using a Bruker APEX II CCD diffractometer which employed graphite-monochromated Mo Kα radiation (λ=0.71073Å) at 100 K. The intensities were obtained *via* ω - 2θ scan mode in the range of $3.1° < \theta < 26.0°$. The structure of the compound was solved directly by the SHELXS-97 program (Sheldrick, 2008) and refined *via* a full matrix least-square method on F^2 using the SHELXL-97 program package (semi-empirical absorption corrections were applied using SADABS program). The melting point of the compound was determined using a capillary melting point apparatus (MEL-TEMP II Laboratory Devices, USA).

3. EXPERIMENTAL

3.1. Chemistry

3.1.1. General Procedure

Three steps were involved in the synthesis of **G4**, whereby the two initial steps Scheme (**1**) were performed to obtain the cyclic compound **2** for use in the third step. In general, 2-(phenylamino)benzoic acid (**1**) and 9-chloroacridine (**2**) were prepared according to the procedure in the literature [19]. The first step involved the Ullmann condensation reaction, whereby 2-chloro benzoic acid and aniline were dissolved in K_2CO_3 in dimethylformamide (DMF). The mixture was refluxed at 136°C overnight under continuous stirring, with copper iodide and copper powder as the catalysts. After compound **1** was formed, it was cyclized by refluxing at 135 – 145 °C for 3 hours with $POCl_3$. Compound **2**, a yellow precipitate, was obtained, which was then purified using concentrated ammonia and crushed ice.

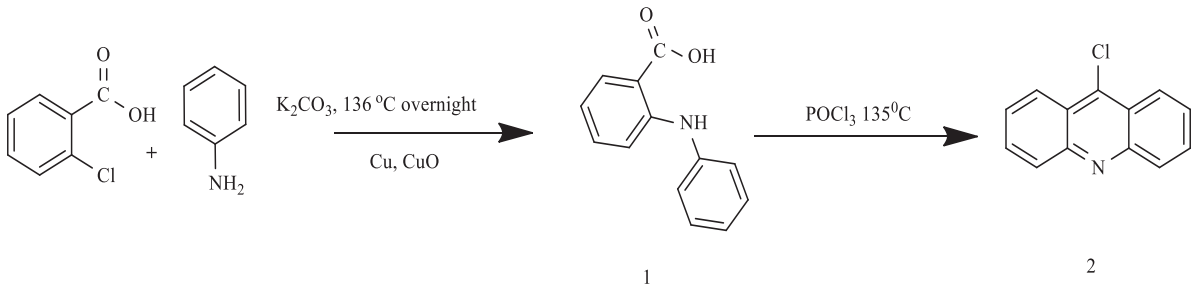

Scheme (1). Synthesis of 9-chloroacridine (**2**)

3.2. Synthesis of *N*-(3,5- Dimethoxyphenyl) Acridin-9-Amine (G4)

Scheme (**2**) outlines the steps of **G4** synthesis using pre-synthesized compound **2**. 3,5-dimethoxyaniline (0.7 g, 4.7 mmol) and potassium carbonate (0.7 g, 4.7 mmol) were dissolved in absolute ethanol (*ca* 20.0 ml). The mixture was stirred for 45 minutes at room temperature, after which compound **2** (0.5 g, 2.3 mmol) and potassium iodide (0.1 g, 0.6 mmol) were added. The mixture was further stirred and refluxed overnight. Upon completion of the reaction, the solvent was evaporated and the remaining solid was poured into 50.0 ml of water and extracted with ethyl acetate. The orange precipitate was filtered out and washed with cold methanol prior to drying. The physical data is listed in (Table **1**).

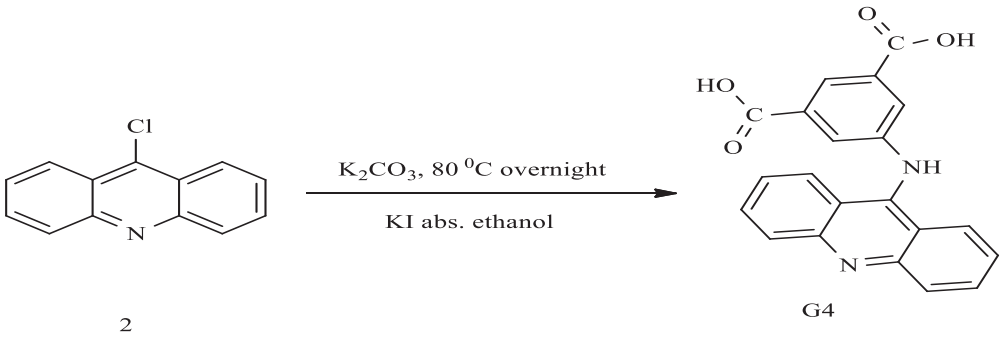

Scheme. (2). Synthesis of *N*-(3,5- dimethoxyphenyl)acridin-9-amine (**G4)**.

Table 1. Physical data for the *N*-(3,5 dimethoxyphenyl)acridin-9-amine, G4.

Compound	Yield (%)	Mp (° C)	Re-crystal Solvent	Crystal Appearance	IR (cm^{-1})
G4	91.8	184.0-186.0	Methanol	Dark red	3358.7 (N-H)
					1614.2 (C=N)
					1170.3 (C-O) (methoxy group)
					1470.3 (C=C)

3.3. Biological Studies

3.3.1. *In Vitro* Cytotoxicity Assay

Cell cultures were maintained in humidified air with 5% CO_2 at 37°C. MTT assay is currently the most commonly-used method to test the cytotoxicity of **G4**. The cells were plated in triplicates on a 96-well plate at a density of 2×10^5 cells/mL in 100 µL of culture medium. Different concentrations of G4 (50, 25, 12.5, 6, 3, and 1.5 µg/mL) were prepared by serial dilution. All serial dilutions were transferred to the cells in the 96-well plates. Untreated cells acted as the control. The cells were incubated for 24 hours, after which their viability was assessed by adding 20 µL of 3-(4,5-dimethylthiazol-2-yl)-2,5-diphenyltetrazolium bromide (MTT, 5 mg/mL) to the cells in a dark room. The cells were then covered with aluminium foil and incubated for another 4 hours. Then, all the media were removed and 100 µL of DMSO added to the cells to solubilize the formazan crystals. Subsequently, the absorbance was read at a wavelength of

570 nm using a microplate reader. The test agents' cell growth inhibition abilities were expressed in terms of IC_{50} (*i.e.* the concentrations at which cell growths were reduced by half).

3.4. Animals

Mice of both genders were obtained from the Animal House Unit, Faculty of Medicine, University of Malaya (UM). All procedures on these animals were carried out in compliance with the regulations designated by the Institutional Animal Care and Use Committee, Faculty of Medicine, UM. The mice were kept in sterilized plastic cages with homogenized wood shavings as bedding. The ambient temperature was maintained at 22 ± 2°C, with 12 hours each of in the light-dark cycle and a relative humidity of 50 – 60%. Food and water were supplied at all times.

3.5. Experimental Animals

Thirty-six mice (18 male and 18 female) were divided into three groups which were labelled as (1) group 1 or vehicle, which was administered 0.5% carboxymethyl cellulose (CMC) at 5 ml/kg; (2) group 2, which was administered 5 ml/kg of **G4** at 500 mg/kg; and (3) group 3, which was administered 5 ml/kg of G4 at 1000 mg/kg. The animals were deprived of food overnight prior to treatment and for 3 – 4 hours after treatment. The purpose of the fasting was to eliminate all the food inside their gastrointestinal tracts that may otherwise complicate the absorption of the tested substance. The mice were monitored for the development of toxicity signs within 48 hours after the intragastrical administration of **G4**. The number of deaths was recorded over 14 consecutive days. On the 15^{th} day, all the mice were killed *via* xylazine-ketamine aesthetic overdose, following which histological (liver and kidney) evaluations and serum analyses were conducted according to the standard techniques [20]

3.6. Assessment of Kidney and Liver Functions

All biochemical assays were performed spectrophotometrically using a Hitachi-912 Autoanalyzer (Mannheim, Germany). Kidney functions were assessed in terms of anion gaps, blood urea nitrogen, as well as serum creatinine, sodium, potassium, chloride, and carbon dioxide levels. Serum Alanine Aminotransferase (ALT), Alkaline Phosphate (ALP), Gamma-Glutamyl Transferase (GGT), albumin, globulin, and bilirubin levels were also measured to evaluate the liver functions. All the serum samples were analysed in a blind manner to obtain data with good sensitivity and validity.

3.7. Assessment of Lipid Profile

The concentrations of total cholesterol and High-Density Lipoprotein (HDL) cholesterol were estimated using the commercial kits by Span Diagnostics in accordance with the method described in the literature [21]. The triglyceride concentrations were assessed by GPO-PAP end-point assay.

3.8. Histopathological Examinations

Renal and hepatic tissues were fixed in 10% formalin and embedded in paraffin, after which they were sectioned at intervals of 5 μm and stained with hematoxylin-eosin solution. All sections were examined photomicroscopically (Olympus BH-2, Japan) by an independent histopathologist who had no knowledge of the treatment groups.

3.9. Measurement of Lipid Peroxidation

The extent of lipid peroxidation was assessed with Malondialdehyde (MDA) as the indicator. Initially, 10% (weight/volume) homogenates of kidney and liver specimens were obtained from 0.1 mol/L phosphate buffer which was centrifuged at 4°C and 3500 rpm for 10 minutes. Then, 0.2 ml of supernatant was mixed with 0.67% 2-Thiobarbituric Acid (TBA) and 20% trichloroacetic acid solutions, followed by heating in a boiling water bath for 30 minutes. The absorbance of the pink chromogen formed by the reaction of TBA with MDA was measured at 532 nm. The results were expressed as MDA nmol/mg protein. The protein contents of the supernatant were measured *via* the Lowry method [22]

3.10. Measurement of Tissue Glutathione

Tissue samples were homogenized in 10 volumes of ice-cold 10% trichloroacetic and then centrifuged at 1000 rpm and 4°C for 15 minutes. The supernatant was removed and re-centrifuged at 35000 rpm and 4°C for 8 minutes.

Glutathione (GSH) levels were determined using a spectrophotometric method, which is a modification of the Ellman procedure [23]

3.11. Statistical Analysis

All data were expressed as means ± SD and analysed using one-way ANOVA followed by post-hoc Tukey HSD multiple comparisons test. The type-1 error level was set $P < 0.05$ for all tests. This entire process was performed using SPSS software (Chicago, IL, USA) version 19.0 for Microsoft Windows.

4. RESULTS AND DISCUSSIONS

4.1. Chemistry

G4 was synthesized *via* one-pot reaction, which began with the reaction between 9-chloroacridine (a ligand) reacted with 3,5-dimethoxyaniline (a aniline substituent) in absolute ethanol, with potassium iodide as the catalyst. The orange precipitate of **G4** was dissolved in methanol, and a few drops of triethylamine added to form solid, dark red, single crystal. This crystal was grown at room temperature. **G4** was characterized by FTIR, ^{1}H, ^{13}C-APT NMR, and elemental analysis. The molecular and crystal structures of **G4** were determined using single crystal X-ray diffraction.

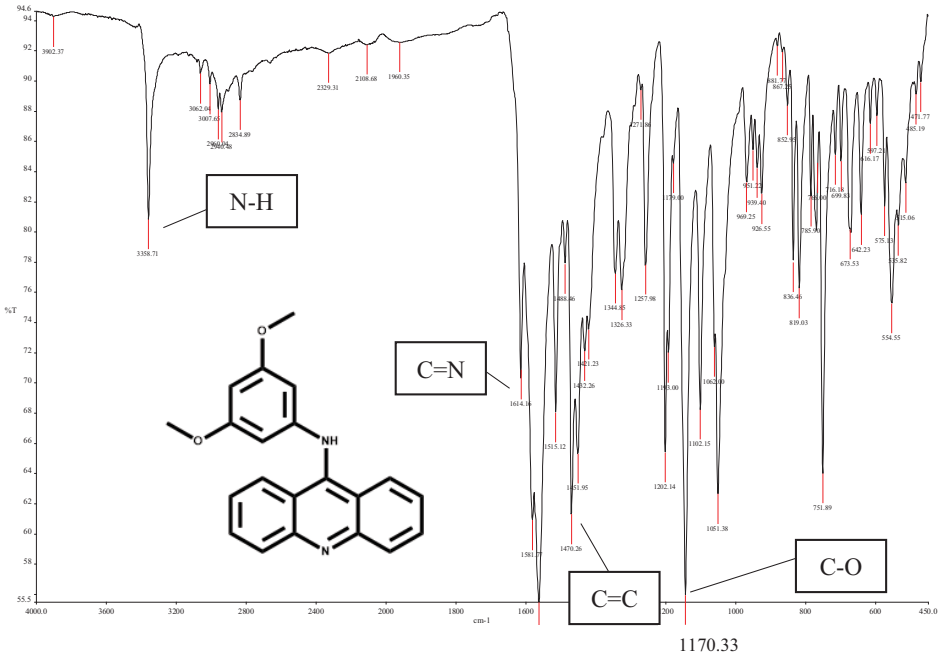

Fig. (1). FTIR spectrum for **G4**.

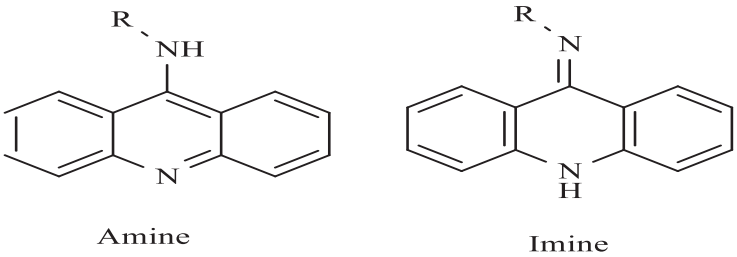

Fig. (2). Two tautomeric forms of 9-aminoacridine.

4.2. Spectroscopic Study

In the FTIR spectrum Fig. (**1**) as listed in Table **1**, the absorption band at 1170.3 cm^{-1} was assigned to the methoxy

group -OCH_3. The presence of aromatic rings in the structure was proven by =C-H sp^2 stretching at 3062.0 cm^{-1} and C=C stretching at 1470.3 cm^{-1}. The absorbance of the -NH group was observed at 3358.7 cm^{-1}, indicating the conversion of the -NH_2 group to –NH. This was consistent with the bond formation between 9-chloroacridine and 3,5-dimethoxy aniline *via* -NH_2 deprotonation.

The ^{1}H NMR Table **2** spectrum of **G4** showed six protons as a singlet at δ 3.64 ppm in two -O-CH_3 groups. The three aromatic rings in **G4** were denoted as multiplets between δ 6.50 and 8.30 ppm. Within these peaks, there were two doublet peaks at δ 8.26 and 8.16 ppm (*i.e.* the most deshielded region) as compared to other -C-H aromatic signals. This was assigned to the four protons of acridine. Meanwhile ^{13}C-APT NMR Table **3** revealed five and seven signals of quaternary and tertiary carbons respectively. The aromatic carbon atoms attached to the methoxy group were denoted at 161.62 ppm, while the methoxy carbon peak was at 55.61 ppm. It was reported that the skeleton of 9-aminoacridine derived from the parent acridine can exist in two tautomeric forms [24] – imine or amine form Fig. (**2**). Tautomerization can occur when different solvents or reaction temperatures are used. Nevertheless, **G4** was observed to be more stable in amine form as proven by the crystal structure.

Table 2. ^{1}H NMR data for G4; chemical shifts in ppm relative to TMS (1%) at room temperature in $CDCl_3$

Compound	Aromatic	O-CH_3
G4	8.26 (d, *J* = 8 Hz; 2H, Ar-H)	3.64 (s, 6H, OCH_3)
-	8.16 (d, *J* = 8 Hz; 2H, Ar-H)	-
-	7.45 (t, *J* = 8 Hz; 2H, Ar-H)	-
-	7.09 (t, *J* = 8 Hz; 2H, Ar-H)	-
-	6.56 (d, *J* = 4 Hz; 2H, Ar-H)	-
-	6.23 (t, *J* = 4 Hz; 1H, Ar-H)	-

Table 3. ^{13}C NMR data for G4; chemical shifts in ppm relative to TMS (1%) at room temperature in $CDCl_3$

Compound	Aromatic (Ar)	O-CH_3	C-N
G4	139.95, 134.49, 126.32, 123.91,	161.62 (Ar-O-CH_3)	142.81, 139.95 (C-N)
	119.76, 114.78, 101.91, 99.07	55.61 (O-CH_3)	154.32 (C-N)

4.3. X-ray Crystallography: Single-crystal X-Ray Diffraction

The structure of **G4** was determined by single crystal X-ray diffraction analysis and is found to be of discrete asymmetric units (Fig. **3**). The crystal data has been deposited to Cambridge Crystallographic Data Centre (CCDC) with the deposition number of CCDC 1587404. The crystallographic data and that of its structure refinement were collected and presented in Table **4**. In the **G4** molecule, 9-acridine (C13) is bound to 3,5-dimethoxyaniline (N1), as expected. The bond lengths and angles (Table **5**) were in agreement with those of other associated derivatives in the literature [25]. The molecule can be divided into two main fragments: (C1-C13/N2) and (N1/C14-C21/O1/O2). The C1-C13/N2 and N1/C14-C21/O1/O2 planes were slightly planar, with a maximum deviation of C13 from the mean plane that was 0.368(2). The dihedral angle between the aforementioned planes was 63.53(6)°. Also, there were no intra- or inter-hydrogen bonds in this molecule (Fig. **4**).

Table 4. Crystal data and structure refinement of G4.

Identification Code	Compound G4 from Methanol
Emprical formula	$C_{21}H_{18}N_2O_2$
Crystal color	Red
Formula weight	330.37
Temperature	293(2) K
Wavelength	1.54178 Å
Crystal system	Orthorhombic
Space group	P212121
a/Å	10.1753(4) Å

(Table 4) contd.....

Identification Code	Compound G4 from Methanol
b/Å	11.8991(5) Å
c/Å	13.4416(6) Å
α/	90.00
β/	90.00
γ/	90.00
Volume/ Å	1627.47(12)
Z	4
ρ_{calc} g/cm^3	1.348 Mg/m
μ/mm^{-1}	0.701 mm
F(000)	696
2θ range for data collection/	4.96 to 73.52
Index ranges	-11<=h<=12, -9<=k<=14, -15<=l<=16
Reflections collected	4381
Independent reflections	2819 [R(int) = 0.0410]
Data/restraints/ parameters	2819 / 0 / 227
Goodness of fit on F2	0.959
Final R indexes [I>=2σ (I)]	R1 = 0.0551, wR2 = 0.1361
Final R indexes [all data]	R1 = 0.0541, wR2 = 0.1406
Largest diff. peak/hole / eÅ-3	0.496 and -0.368

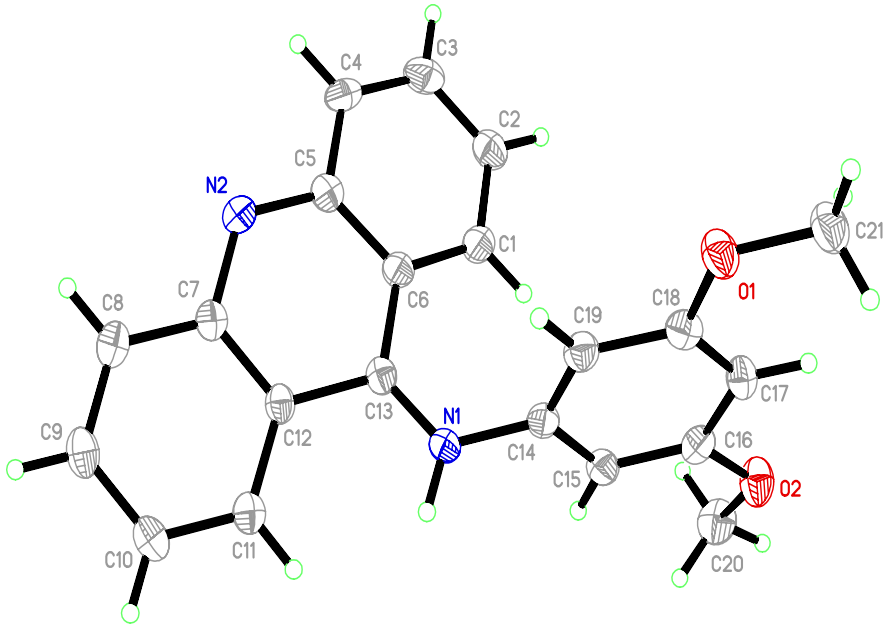

Fig. (3). The ORTEP diagram of **G4**, showing 50% probability displacement ellipsoids and the atom-numbering scheme.

Table 5. Selected bond length (Å) and angles (°).

Bond	Bond Lengths	Bond	Bond Angle
C13-N1	1.287(3)	C13-N1-C14	123.0(2)
C14-N1	1.407(3)	C18-O1-C21	116.8(2)
C18-O1	1.369(3)	C16-O2-C20	117.2(2)
C16-O2	1.354(3)	N1-C13-C6	126.9(2)

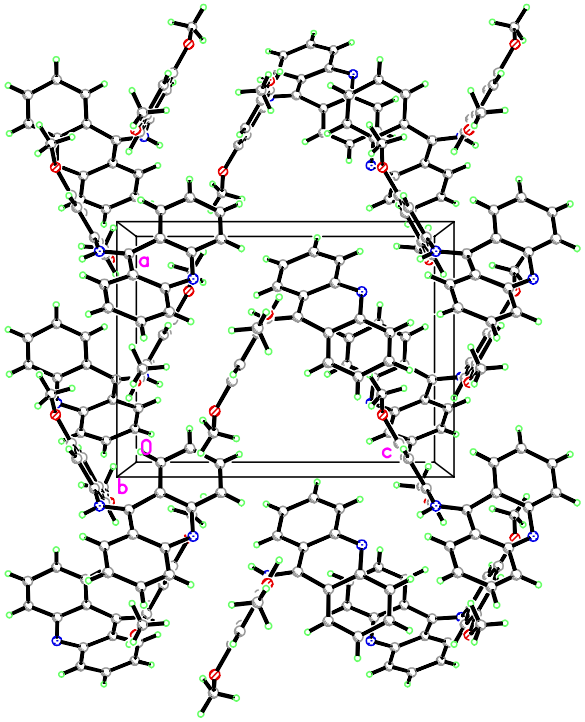

Fig. (4). The packing of **G4 as** viewed down to the *b* axis.

5. BIOLOGICAL

5.1. Anti-proliferative Activity of G4

The effects of **G4** on the viability of MCF-7, HL60, HT29, and WRL68 cells were measured using MTT assay. Following 24 hours of exposure to **G4**, there was a significant inhibition of cellular proliferation in the treated cells as compared to the non-treated cells (controls). Among the tested cells, HL-60 gave the best results with an IC_{50} of 15 ± 0.03 Table **6**. The present study has shown that the cytotoxic activities of **G4** on MCF-7, HT29, and HL60 cells were high while that of WRL68 was very low. The findings suggested that **G4** is a potential candidate for further anticancer studies.

Table 6. Cytotoxicities of G4 in MTT assay.

Cell Line	WRL68	MCF-7	HT29	HL60
IC_{50} (µg/ml)	49 ± 0.05	22 ± 0.04	17.5 ± 0.02	15 ± 0.03

5.2. General Acute Toxicity Observation

The acute toxicity study was carried out to determine a nontoxic dose of **G4**. After fourteen days of the intragastrical administration of two different concentrations of **G4**, no behavioural alterations or deaths were observed. In the mice, **G4** did not show any abnormalities in terms of their behaviours or physical appearances. Food and water were provided as usual, and the faeces of the mice were dark and dry. There were no significant differences in the body weights of the mice as well.

Table 7. Serum biochemical data for male and female mice orally administered G4 at different concentrations for 14 days.

Parameters	Sex	Control mean ± SD	500 mg/kg mean ± SD	1000 mg/kg mean ± SD
Sodium mmol/L	Male	151±1.22	152±0.23	152.6±3.13
	Female	149±0.55	149.6±0.54	149±2.5
Potassium mmol/L	Male	5.8±0.5	4.6±1.4	5.01±0.39
	Female	4±0.7	4.84±0.5	4±1.21
Chloride mmol/L	Male	108.8±1.64	107±0.2	107.6±2.3
	Female	110±2.7	110.2±1.1	109±0.68
Carbon Dioxide mmol/L	Male	13.4±4.5	13±2.1	13.6±2.9
	Female	19±2.41	18±2.9	19±3.2

(Table 7) contd.....

Parameters	Sex	Control mean ± SD	500 mg/kg mean ± SD	1000 mg/kg mean ± SD
Anion Gap mmol/L	Male	34.8±3.8	33.7±0.9	35.2±2.4
	Female	27±0.55	27±0.11	28.1±1.89
Urea nitrogen mmol/L	Male	8.26±0.7	9±0.76	8.86±1.32
	Female	8±0.8	8.8±1.3	8.6±1.2
Creatinine mmol/L	Male	8±0	8±0	8±0
	Female	9±0.5	9±0.2	8±0.23
Albumin g/L	Male	27.2±2.6	28±3.1	27±1.2
	Female	27±1.7	27±0.24	28±3.1
Total Bilirubin umol/L	Male	1±0	1±0	1.4±0.55
	Female	1±0.2	1±0.23	1±0.9
Alkaline Phosphatase IU/L	Male	61.4±0.5	74±0	75.2±8.6
	Female	67±6.5	68±4.1	66.5±3.7
Alanine Aminotransferase IU/L	Male	41.6±0.9	41.1±6.7	42.6±3.2
	Female	34.01±5.3	33.1±0	33.4±1.3
G-Glutamyal Transferase IU/L	Male	4.6±3.2	4±0.6	4.4±1.82
	Female	2±0.3	2±0.21	3±0.15

5.3. Serum Biochemical Parameters

All mice that were treated with either 500 or 1000 mg/kg of **G4** did not exhibit significant differences in the levels of their liver function markers (albumin, total bilirubin, ALP, ALT, and GGT). Table **7**. contains the data on serum biochemistry. There were also no significant changes in the renal profiles (potassium, chloride, sodium, and urea) of the mice. For the mice dosed with 500 mg/kg of **G4**, there were significant increases in the total cholesterol, HDL cholesterol, LDL cholesterol, and triglyceride levels of all mice except for the triglyceride level for male mice that is slightly decreased. As for the mice treated with 1000 mg/kg of **G4**, in male mice, the triglyceride and total cholesterol levels were decreased while in female mice the reduced amount of LDL cholesterol level was observed. On the other hand, the HDL cholesterol level for all mice, the triglyceride level for only female mice and LDL cholesterol level for male mice were found to be increasing. Nevertheless, the total cholesterol level on female mice was unchanged as compared to the control mice. The effects of **G4** on the lipid profile are shown in Table (**8**).

Table 8. Effect of G4 on triglycerides, total cholesterol, HDL cholesterol, and LDL cholesterol.

Parameters (mmol/L)	Sex	Control mean ± SD	500 mg/kg mean ± SD	1000 mg/kg mean ± SD
Triglyceride	Male	1.54±0.32	1.39±0.33	1.16±0.5
	Female	1.5±0.4	1.8±0.07	1.7±0.41
Total Cholesterol	Male	2.92±0.41	3.1±0.8	2.78±0.3
	Female	2±0.1	2.4±0.13	2±0.19
HDL Cholesterol	Male	1.66±0.32	1.8±0.9	1.94±0.5
	Female	0.9±0.27	2.4±0.13	1.2±0.26
LDL Cholesterol	Male	1.21±0.2	1.13±0.69	1.48±0.72
	Female	1.53±0.1	1.67±0.74	1.37±0.49

5.4. Histopathological Evaluation

The kidney and liver examinations of mice did not show any abnormalities in terms of gross appearance and weight as a result of **G4** consumption. The results of gross examination were also confirmed by histopathological assessment. There were no detected ions of any damage in their gastroinstestinal tracts or the potential and direct target for toxic effects of the ingested foods. **G4** was also not responsible for any significant histological changes in the mice Fig. (**5**). Hence, it can be concluded that there was no necrosis, cirrhosis, and inflammation. These outcomes revealed that intragastric **G4** up to a concentration of 1000 mg/kg was not toxic to mice.

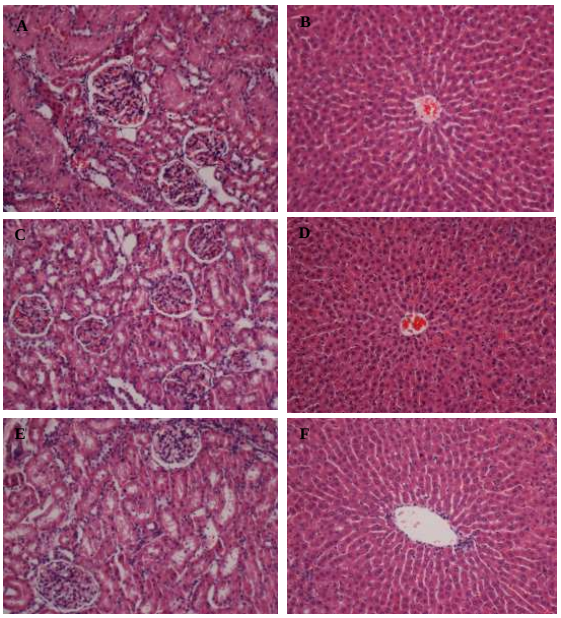

Fig. (5). Effect of **G4** on histological sections of the liver and kidney in mice. (A, B) Mice treated with vehicle. (C, D) Mice treated with 500 mg/kg of **G4**. (E, F) Mice treated with 1000 mg/kg of **G4**. There are no significant differences in the architectures of the livers and kidneys between the treatment and control groups (H & E stain, 20× magnification).

CONCLUSION

The acridine was observed to be bound to 3,5-dimethoxyaniline (N1) as the confirmed **G4** molecule. Also, the exocyclic carbon at position C13 was found to be monodentate and slightly planar. **G4** exhibited profound antiproliferative activity towards HL60 cancer cell lines. Intragastrical administration of up to 1000 mg/kg of **G4** did not result in toxicity effects to the mice. The anticancer mechanism of **G4** can be further investigated *in vitro* and *in vivo* since there is evidence for its potential to be developed into new pharmaceutical drugs.

CONSENT FOR PUBLICATION

Not applicable.

CONFLICT OF INTEREST

The authors declare no conflict of interest, financial or otherwise.

ACKNOWLEDGEMENTS

This work was supported by the University of Malaya IPPP Grant; Grant No. PG107-2016A and Grant No. RACE CR011-2015. Special thanks to Dr Mohd Ridzuan Mohd Abd Razak of Institute for Medical Research (IMR), Kuala Lumpur for his help in biological evaluation write-up.

REFERENCES

[1] (a) Korth, C.; May, B.C.; Cohen, F.E.; Prusiner, S.B. Acridine and phenothiazine derivatives as pharmacotherapeutics for prion disease. *Proc. Natl. Acad. Sci. USA,* **2001**, *98*(17), 9836-9841. [http://dx.doi.org/10.1073/pnas.161274798] [PMID: 11504948] (b) Kumar, A.; Kumar, N.; Roy, P.; Sondhi, S.M.; Sharma, A. Synthesis of acridine cyclic imide hybrid molecules and their evaluation for anticancer activity. *Med. Chem. Res.,* **2015**, *24*(8), 3272-3282. [http://dx.doi.org/10.1007/s00044-015-1380-2]

[2] (a) Temple, M.D.; McFadyen, W.D.; Holmes, R.J.; Denny, W.A.; Murray, V. Interaction of cisplatin and DNA-targeted 9-aminoacridine platinum complexes with DNA. *Biochemistry,* **2000**, *39*(18), 5593-5599. [http://dx.doi.org/10.1021/bi9922143] [PMID: 10820033] (b) Maresca, L.; Pacifico, C.; Pappadopoli, M.C.; Natile, G. Endocyclic versus exocyclic N-coordination to platinum(II) of some nitro-9-[(2-dialkylaminoethyl)amino]acridines. *Inorg. Chim. Acta,* **2000**, *304*(2), 274-282. [http://dx.doi.org/10.1016/S0020-1693(00)00100-6]

[3] (a) Riera, X.; Moreno, V.; Ciudad, C.J.; Noe, V.; Font-Bardía, M.; Solans, X. Complexes of Pd(II) and Pt(II) with 9-aminoacridine: Reactions with DNA and study of their antiproliferative activity. *Bioinorg. Chem. Appl.,* **2007**, *2007*, 98732. [http://dx.doi.org/10.1155/2007/98732] [PMID: 18364995] (b) Ruiz, J.; Lorenzo, J.; Vicente, C.; López, G.; María López-de-Luzuriaga, J.;

Monge, M.; Avilés, F.X.; Bautista, D.; Moreno, V.; Laguna, A. New palladium(II) and platinum(II) complexes with 9-aminoacridine: structures, luminiscence, theoretical calculations, and antitumor activity. *Inorg. Chem.,* **2008**, *47*(15), 6990-7001. [http://dx.doi.org/10.1021/ic800589m] [PMID: 18593114]

[4] Pang, X.; Chen, C.; Su, X.; Li, M.; Wen, L. Diverse tandem cyclization reactions of o-cyanoanilines and diaryliodonium salts with copper catalyst for the construction of quinazolinimine and acridine scaffolds. *Org. Lett.,* **2014**, *16*(23), 6228-6231. [http://dx.doi.org/10.1021/ol503156g] [PMID: 25420123]

[5] (a) Borovlev, I.V.; Demidov, O.P.; Amangasieva, G.A.; Avakyan, E.K. Direct and facile synthesis of 9-aminoacridine and acridin-9-yl-ureas. *Tetrahedron Lett.,* **2016**, *57*(32), 3608-3611. [http://dx.doi.org/10.1016/j.tetlet.2016.06.103] (b) Sondhi, S.M.; Kumar, S.; Rani, R.; Chakraborty, A.; Roy, P. Synthesis of Bis-acridine Derivatives Exhibiting Anticancer and Anti-inflammatory Activity. *J. Heterocycl. Chem.,* **2013**, *50*(2), 252-260. [http://dx.doi.org/10.1002/jhet.985]

[6] (a) Di Giorgio, C.; Nikoyan, A.; Decome, L.; Botta, C.; Robin, M.; Reboul, J-P.; Sabatier, A-S.; Matta, A.; De Méo, M. DNA-damaging activity and mutagenicity of 16 newly synthesized thiazolo [5,4-a]acridine derivatives with high photo-inducible cytotoxicity. *Mutat. Res.,* **2008**, *650*(2), 104-114. [http://dx.doi.org/10.1016/j.mrgentox.2007.10.022] [PMID: 18160333] (b) Ketron, A.C.; Denny, W.A.; Graves, D.E.; Osheroff, N. Amsacrine as a topoisomerase II poison: Importance of drug-DNA interactions. *Biochemistry,* **2012**, *51*(8), 1730-1739. [http://dx.doi.org/10.1021/bi201159b] [PMID: 22304499] (c) Loza-Mejía, M.A.; Castillo, R.; Lira-Rocha, A. Molecular modeling of tricyclic compounds with anilino substituents and their intercalation complexes with DNA sequences. *J. Mol. Graph. Model.,* **2009**, *27*(8), 900-907. [http://dx.doi.org/10.1016/j.jmgm.2009.02.001] [PMID: 19269869] (d) Bacherikov, V.A.; Chang, J-Y.; Lin, Y-W.; Chen, C-H.; Pan, W-Y.; Dong, H.; Lee, R-Z.; Chou, T-C.; Su, T-L. Synthesis and antitumor activity of 5-(9-acridinylamino)anisidine derivatives. *Bioorg. Med. Chem.,* **2005**, *13*(23), 6513-6520. [http://dx.doi.org/10.1016/j.bmc.2005.07.018] [PMID: 16140018]

[7] Cuzick, J.; Sestak, I.; Cawthorn, S.; Hamed, H.; Holli, K.; Howell, A.; Forbes, J.F. Tamoxifen for prevention of breast cancer: extended long-term follow-up of the IBIS-I breast cancer prevention trial. *Lancet Oncol.,* **2015**, *16*(1), 67-75. [http://dx.doi.org/10.1016/S1470-2045(14)71171-4] [PMID: 25497694]

[8] (a) de Martel, C.; Ferlay, J.; Franceschi, S.; Vignat, J.; Bray, F.; Forman, D.; Plummer, M. Global burden of cancers attributable to infections in 2008: A review and synthetic analysis. *Lancet Oncol.,* **2012**, *13*(6), 607-615. [http://dx.doi.org/10.1016/S1470-2045(12)70137-7] [PMID: 22575588] (b) Plummer, M.; de Martel, C.; Vignat, J.; Ferlay, J.; Bray, F.; Franceschi, S. Global burden of cancers attributable to infections in 2012: A synthetic analysis. *Lancet Glob. Health,* **2016**, *4*(9), e609-e616. [http://dx.doi.org/10.1016/S2214-109X(16)30143-7] [PMID: 27470177]

[9] Amit Tiwari, N.G.K.; Kumar, N.; Kumar, N.; Chaudhary, A.; Vasanth R., P.; Shenoy, R.; Rao, C. M. *Synthesis and evaluation of selected 1,3,4 oxadiazolebderivatives for in vitro cytotoxicity and in vivo anti-tumor activity*; Springer Science Cytotechnology, **2016**, pp. 1-13. (b) Mohammadi-Khanaposhtani, M.; Safavi, M.; Sabourian, R.; Mahdavi, M.; Pordeli, M.; Saeedi, M.; Ardestani, S.K.; Foroumadi, A.; Shafiee, A.; Akbarzadeh, T. Design, synthesis, *in vitro* cytotoxic activity evaluation, and apoptosis-induction study of new 9(10H)-acridinone-1,2,3-triazoles. *Mol. Divers.,* **2015**, *19*(4), 787-795. [http://dx.doi.org/10.1007/s11030-015-9616-0] [PMID: 26170096]

[10] (a) Janočková, J.; Plšíková, J.; Kašpárková, J.; Brabec, V.; Jendželovský, R.; Mikeš, J.; Kovaľ, J.; Hamuľaková, S.; Fedoročko, P.; Kuča, K.; Kožurková, M. Inhibition of DNA topoisomerases I and II and growth inhibition of HL-60 cells by novel acridine-based compounds. *Eur. J. Pharm. Sci.,* **2015**, *76*, 192-202. [http://dx.doi.org/10.1016/j.ejps.2015.04.023] [PMID: 25960253] (b) Wang, Y.; Gao, D.; Chen, Z.; Li, S.; Gao, C.; Cao, D.; Liu, F.; Liu, H.; Jiang, Y. Acridone derivative 8a induces oxidative stress-mediated apoptosis in CCRF-CEM leukemia cells: Application of metabolomics in mechanistic studies of antitumor agents. *PLoS One,* **2013**, *8*(5), e63572. [http://dx.doi.org/10.1371/journal.pone.0063572] [PMID: 23667640] (c) Gao, H.; Denny, W.A.; Garg, R.; Hansch, C. Quantitative structure-activity relationships (QSAR) for 9-anilinoacridines: A comparative analysis. *Chem. Biol. Interact.,* **1998**, *116*(3), 157-180. [http://dx.doi.org/10.1016/S0009-2797(98)00085-4] [PMID: 9920460]

[11] (a) Wainwright, M. Acridine-a neglected antibacterial chromophore. *J. Antimicrob. Chemother.,* **2001**, *47*(1), 1-13. [http://dx.doi.org/10.1093/jac/47.1.1] [PMID: 11152426] (b) Benoit, A.R.; Schiaffo, C.; Salomon, C.E.; Goodell, J.R.; Hiasa, H.; Ferguson, D.M. Synthesis and evaluation of N-alkyl-9-aminoacridines with antibacterial activity. *Bioorg. Med. Chem. Lett.,* **2014**, *24*(14), 3014-3017. [http://dx.doi.org/10.1016/j.bmcl.2014.05.037] [PMID: 24908610]

[12] Gamage, S.A.; Figgitt, D.P.; Wojcik, S.J.; Ralph, R.K.; Ransijn, A.; Mauel, J.; Yardley, V.; Snowdon, D.; Croft, S.L.; Denny, W.A. Structure-activity relationships for the antileishmanial and antitrypanosomal activities of 1′-substituted 9-anilinoacridines. *J. Med. Chem.,* **1997**, *40*(16), 2634-2642. [http://dx.doi.org/10.1021/jm970232h] [PMID: 9258370]

[13] (a) Auparakkitanon, S.; Wilairat, P. Cleavage of DNA induced by 9-anilinoacridine inhibitors of topoisomerase II in the malaria parasite Plasmodium falciparum. *Biochem. Biophys. Res. Commun.,* **2000**, *269*(2), 406-409. [http://dx.doi.org/10.1006/bbrc.2000.2305] [PMID: 10708566] (b) Prajapati, S.P.; Kaushik, N.K.; Zaveri, M.; Mohanakrishanan, D.; Kawathekar, N.; Sahal, D. Synthesis, characterization and antimalarial evaluation of new β-benzoylstyrene derivatives of acridine. *Arab. J. Chem.,* **2012**.

[14] (a) Rubio-Pons, Ò.; Serrano-Andrés, L.; Merchán, M. A theoretical insight into the photophysics of acridine. *J. Phys. Chem. A,* **2001**, *105*(42), 9664-9673. [http://dx.doi.org/10.1021/jp013124m] (b) Dai, Y.; Xu, K.; Li, Q.; Wang, C.; Liu, X.; Wang, P. Acridine-based complex as amino acid anion fluorescent sensor in aqueous solution. *Spectrochim. Acta A Mol. Biomol. Spectrosc.,* **2016**, *157*, 1-5.

[http://dx.doi.org/10.1016/j.saa.2015.12.007] [PMID: 26687098] (c) Zhang, Y.; Pan, J.; Zhang, G.; Zhou, X. Intercalation of herbicide propyzamide into DNA using acridine orange as a fluorescence probe. *Sens. Actuators B Chem.,* **2015**, *206*, 630-639. [http://dx.doi.org/10.1016/j.snb.2014.09.114]

[15] Mondek, J.; Mravec, F.; Halasová, T.; Hnyluchová, Z.; Pekař, M. Formation and dissociation of the acridine orange dimer as a tool for studying polyelectrolyte-surfactant interactions. *Langmuir,* **2014**, *30*(29), 8726-8734. [http://dx.doi.org/10.1021/la502011s] [PMID: 25001412]

[16] (a) Mukherjee, N.; Podder, S.; Banerjee, S.; Majumdar, S.; Nandi, D.; Chakravarty, A.R. Targeted photocytotoxicity by copper(II) complexes having vitamin B6 and photoactive acridine moieties. *Eur. J. Med. Chem.,* **2016**, *122*, 497-509. [http://dx.doi.org/10.1016/j.ejmech.2016.07.003] [PMID: 27423638] (b) Fahrenholtz, C.D.; Ding, S.; Bernish, B.W.; Wright, M.L.; Zheng, Y.; Yang, M.; Yao, X.; Donati, G.L.; Gross, M.D.; Bierbach, U.; Singh, R. Design and cellular studies of a carbon nanotube-based delivery system for a hybrid platinum-acridine anticancer agent. *J. Inorg. Biochem.,* **2016**, *165*, 170-180. [http://dx.doi.org/10.1016/j.jinorgbio.2016.07.016] [PMID: 27496614]

[17] Liu, Y.; Aghdassi, N.; Wang, Q.; Duhm, S.; Zhou, Y.; Song, B. Solvent-resistant ITO work function tuning by an acridine derivative enables high performance inverted polymer solar cells. *Org. Electron.,* **2016**, *35*, 6-11. [http://dx.doi.org/10.1016/j.orgel.2016.04.041]

[18] Kostrhunova, H.; Malina, J.; Pickard, A.J.; Stepankova, J.; Vojtiskova, M.; Kasparkova, J.; Muchova, T.; Rohlfing, M.L.; Bierbach, U.; Brabec, V. Replacement of a thiourea with an amidine group in a monofunctional platinum-acridine antitumor agent. Effect on DNA interactions, DNA adduct recognition and repair. *Mol. Pharm.,* **2011**, *8*(5), 1941-1954. [http://dx.doi.org/10.1021/mp200309x] [PMID: 21806015]

[19] (a) Lang, X.; Li, L.; Chen, Y.; Sun, Q.; Wu, Q.; Liu, F.; Tan, C.; Liu, H.; Gao, C.; Jiang, Y. Novel synthetic acridine derivatives as potent DNA-binding and apoptosis-inducing antitumor agents. *Bioorg. Med. Chem.,* **2013**, *21*(14), 4170-4177. [http://dx.doi.org/10.1016/j.bmc.2013.05.008] [PMID: 23735826] (b) Li, B.; Gao, C-M.; Sun, Q-S.; Li, L-L.; Tan, C-Y.; Liu, H-X.; Jiang, Y-Y. Novel synthetic acridine-based derivatives as topoisomerase I inhibitors. *Chin. Chem. Lett.,* **2014**, *25*(7), 1021-1024. [http://dx.doi.org/10.1016/j.cclet.2014.03.028]

[20] (a) Ibrahim, M.Y.; Abdul, A.B.; Ibrahim, T.A.T.; Abdelwahab, S.I.; Elhassan, M.M.; Syam, M.M. Evaluation of acute toxicity and the effect of single injected doses of zerumbone on the kidney and liver functions in Sprague Dawley rats. *Afr. J. Biotechnol.,* **2010**, *9*(28), 4442-4450. (b) Ibrahim, M.Y.; Hashim, N.M.; Mohan, S.; Abdulla, M.A.; Abdelwahab, S.I.; Arbab, I.A.; Yahayu, M.; Ali, L.Z.; Ishag, O.E. α-Mangostin from Cratoxylum arborescens: an *in vitro* and *in vivo* toxicological evaluation. *Arab. J. Chem.,* **2015**, *8*(1), 129-137. [http://dx.doi.org/10.1016/j.arabjc.2013.11.017]

[21] Wybenga, D.R.; Pileggi, V.J.; Dirstine, P.H.; Di Giorgio, J. Direct manual determination of serum total cholesterol with a single stable reagent. *Clin. Chem.,* **1970**, *16*(12), 980-984. [PMID: 4098216]

[22] Lowry, O.H.; Rosebrough, N.J.; Farr, A.L.; Randall, R.J. Protein measurement with the Folin phenol reagent. *J. Biol. Chem.,* **1951**, *193*(1), 265-275. [PMID: 14907713]

[23] Ellman, G.L. Tissue sulfhydryl groups. *Arch. Biochem. Biophys.,* **1959**, *82*(1), 70-77. [http://dx.doi.org/10.1016/0003-9861(59)90090-6] [PMID: 13650640]

[24] Carlone, M.; Di Masi, N.G.; Maresca, L.; Margiotta, N.; Natile, G. Role of metal ions and hydrogen bond acceptors in the tautomeric equilibrium of nitro-9 [(alkylamino)amino]-acridine drugs. *Bioinorg. Chem. Appl.,* **2004**, *2*(1-2), 93-104. [http://dx.doi.org/10.1155/S156536330400007X] [PMID: 18365071]

[25] (a) Jimenez, M.B.; Gonzalez, F.S.; Caballero, M.C. Crystal structure of dimethyl 5-(acridin-9-yloxy) isophthalate-methanol (1: 1), C23H17NO5· CH3OH. *Z. Kristallogr., New Cryst. Struct.,* **2009**, *224*(4), 603-604. [http://dx.doi.org/10.1524/ncrs.2009.0265] (b) Solovyeva, E.V.; Starova, G.L.; Myund, L.A.; Denisova, A.S. X-ray, IR and Raman study of Ag (I), Cu (II) and Cd (II) complexes with 4, 5-bis (N, N-di (2-hydroxyethyl) iminomethyl) acridine. *Polyhedron,* **2016**, *106*, 1-9. [http://dx.doi.org/10.1016/j.poly.2015.12.049]